Passive Robotic Walker Path Following with Bang-Bang Hybrid Control Paradigm

Marco Andreetto, Stefano Divan, Daniele Fontanelli and Luigi Palopoli

***Abstract*— This paper presents a control algorithm that steers a robotic walking assistant along a planned path using electromechanical brakes. The device is modeled as a Dubins' car, i.e., a wheeled vehicle that moves only forward in the plane and has a limited turning radius. In order to reduce the cost of the hardware, no force sensor is employed. This feature hampers the application of control algorithms based on a modulated braking action. A viable solution is based on the application of on/off braking action, thus forcing the vehicle to turn with a fixed turning radius. In order to avoid the annoying chattering behaviour, which is the inevitable companion of all bang-bang solutions, we propose a hybrid controller based on three discrete states that rule the application of the braking action. The resulting feedback controller secures a gentle convergence of the user toward the planned path and his/her steady progress towards the destination. This is obtained by using two independent hystereses thresholds, the first one associated with the *approaching* phase and the second with the *following* phases. The system convergence toward the path is formally proved. Simulations and experiments show the effectiveness of the proposed approach and the good level of comfort for the user.**

I. Introduction

As a consequence of the constant ageing of the population of advanced countries, an increasing number of senior citizens are facing the difficulties of independent living when deficiencies, sensory or cognitive, or disabilities of different kind appear in their lives [1], [2]. One of the worst effects of physical and cognitive decline is a reduced level of mobility. The use of robots to counter the negative effects of ageing is a strategy with recognised benefits in improving mobility and extending independent living. The *FriWalk* robotic walker developed in the context fo the European Commission ACANTO project [3] combines the benefits of standard walkers (improved stability and physical support) with sensing and computing ability that allow the robot to localise itself and generate safe paths for the user.

The so-called *passive robotics* [4] proposes the use of robots to help people move along desired paths. Known applications can be found in the area of manufacturing [5] and of assistance of people with mobility deficits [6]. Another example is the Cobot walking assistant proposed in [7], which is composed of a cane with a controlled caster wheel that guides the user along a desired path. With Cobots, it is possible to estimate user gait, to guide her preventing falls [8] or to assist leg motions in the swing phase in cooperation with wearable walking support systems [9]. Walking aids proposed in the literature range from steering–only controlled walkers to fully–actuated assistant carts or wheelchairs [10]. A very significant step toward an improved safety has been the outright removal of driving motors [11]. Driving motors can effectively be replaced with electromagnetic brakes mounted on the rear wheels preserving a good level of guidance abilities through a differential control strategy [12]. By suitably modulating the braking torque applied to each wheel, the walker is steered toward the desired path [13], [14]. This paradigm has been also adopted by Fontanelli et al. [15], [16], in the form of an optimal control minimising the braking torques. The literature solutions discussed above have a common drawback: the control laws rely on real–time measurements of the torques applied to the walker, which are difficult to estimate with the desired level of accuracy without expensive sensors. Moreover, the use of electromechanical brakes makes the braking action difficult to be modulated.

One way to tackle this problem is by a bang-bang actuation strategy with saturated inputs: to steer left or right, the controller has to block, respectively and alternatively, the left or right wheel. Clearly, the use of a fixed curvature radius vehicle produces trajectories that may be perceived as uncomfortable for the user, however this disadvantage is implicit in the impossibility of modulating the brakes. A control law with discontinuous input can be defined without a precise knowledge of the torques exerted by the user on the vehicle and with the simple information of position and orientation with respect to the path. The use of saturated input determines a limited curvature radius, as for a Dubins' car. The control solution for a Dubins' car proposed in [17], is based on a discontinuous angular velocity input. This approach has been further developed in [18] for optimal route tracking control by minimising the approaching path length using a hybrid controller. The same authors proposed in [19] an optimal controller to track generic paths with proper curvature that are unknown upfront by considering the curvature of the path as an external disturbance to be rejected. As discussed below, the application of this strategy comes along with an a chattering behaviour in the braking action whenever the walker has to perfectly track generic curvature paths. This effect is very annoying for the user, making the whole solution hardly applicable in our domain.

Our strategy to solve the problem is based on a hybrid

This project has received funding from the European Unions Horizon 2020 Research and Innovation Programme - Societal Challenge 1 (DG CONNECT/H) under grant agreement n° 643644 "ACANTO - A CyberphysicAl social NeTwOrk using robot friends".

D. Fontanelli is with the Department of Industrial Engineering (DII), University of Trento, Via Sommarive 5, Trento, Italy daniele.fontanelli@unitn.it. M. Andreetto, S. Divan and L. Palopoli are with the Department of Information Engineering and Computer Science (DISI), University of Trento, Via Sommarive 5, Trento, Italy {luigi.palopoli,stefano.divan,marco.andreetto}@unitn.it

Fig. 1. The *FriWalk* prototype used for experimental testing.

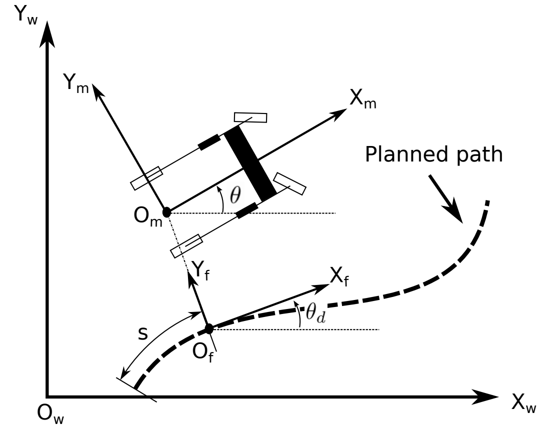

Fig. 2. Vehicle to path configuration and reference frames.

controller, which is formalised and analysed in the paper. Its application allows reducing the control authority and avoiding the chattering phenomenon. At the same time the convergence is guaranteed. The controller is based on the definition of a safety region around the desired path, where corrective actions simply do not occur. In addition, we reduce the number of braking actions by defining suitable path approaching trajectories, controlled in feedback up to a certain tolerance. The proposed hybrid controller has been successfully applied to a real walker and its effectiveness has been proved through extensive experiments.

The paper is organised as follows. In Section II we introduce the most important definitions and state the problem in formal terms. In Section III, we briefly present the extension of literature results to the problem at hand, while Section IV formalises the hybrid solution, with its tuning parameters. Section V presents the simulative and experimental results on the *FriWalk*, and finally Section VI we state our conclusions and announce future work directions.

II. Background and Problem Formulation

The *FriWalk* prototype used for this paper is visible in Fig. 1 and is simply derived from a commercial walker mounting electro-mechanical brakes on the rear wheels. In order to solve the localisation problem, the rear wheels host incremental encoders, which are used in combination with an inertial platform measuring the accelerations and angular velocities and with a camera system [20], [21]. The vehicle uses RGB-D technologies to gather information from the surrounding environment by detecting unexpected and moving obstacles and dangerous surfaces. These information are then used to plan the safest path for the user [22], [23]. In view of the described features, we will assume the presence of two external modules that: 1. generate the reference path, 2. localize the vehicle with a good accuracy (error below 20cm).

A. Vehicle Kinematic Model

Since the front wheels of the robot in Figure 1 are casters, the vehicle is modeled as a unicycle.

With reference to Fig. 2, let $\langle W\rangle = \{O_w,\, X_w,\, Y_w,\, Z_w\}$ be a fixed right-handed reference frame, whose plane $\Pi = X_w \times Y_w$ is the plane of motion of the cart, Z_w pointing outwards the plane Π and let O_w be the origin of the reference frame. Let $\chi = [x,\, y,\, \theta]^T \in \mathbb{R}^2 \times S$ be the kinematic configuration of the cart, where $(x,\, y)$ are the coordinates of the mid–point of the rear wheels axle in Π and θ is the orientation of the vehicle w.r.t. the X_w axis (see Fig. 2). The kinematic model of the unicycle is

$$\dot{\chi} = \begin{bmatrix} \dot{x} \\ \dot{y} \\ \dot{\theta} \end{bmatrix} = \begin{bmatrix} \cos(\theta) & 0 \\ \sin(\theta) & 0 \\ 0 & 1 \end{bmatrix} \begin{bmatrix} v \\ \omega \end{bmatrix}, \qquad (1)$$

where v and ω are the inputs of the unicycle and represent, respectively, the forward velocity and the angular velocities of the vehicle.

In order to perform the path–following problem, a customary assumption is to use a Frenet frame $\langle F\rangle$, which moves along the path following the unicycle dynamic (see Fig. 2). Let s be the curvilinear abscissa parametrising the path, l is the distance along the Y-axis of the Frenet frame between the origin of the Frenet frame and the reference point of the *FriWalk*, and θ_d is the angle between the X_w-axis and the X-axis of the Frenet frame (see Fig. 2). Therefore, $\tilde{\theta} = \theta - \theta_d$. Thanks to this new set of coordinates it is possible to express the kinematic model of the unicycle by means of the diffeomorphism $\zeta = [s, l, \tilde{\theta}] = \Phi(\chi)$ as

$$\dot{\zeta} = \begin{bmatrix} \dot{s} \\ \dot{l} \\ \dot{\tilde{\theta}} \end{bmatrix} = \begin{bmatrix} v\cos(\tilde{\theta})/(1 - c(s)l) \\ v\sin(\tilde{\theta}) \\ \tilde{\omega} \end{bmatrix}, \qquad (2)$$

where $\tilde{\omega} = \omega - c(s)\dot{s}$ and the path curvature is defined as $c(s) = d\theta_d(s)/ds$. A complete derivation of the rather customary model (2), can be found in [24].

B. Problem Formulation

The focus of this paper is to steer the walker acting on the rear brakes in order to converge to a planned path defined in the plane of motion Π. Convergence is defined with respect to a safety tunnel, that can be made arbitrarily small [25], and centered around the desired path. More formally, with respect to the system (2), we seek a control law such that

$$\lim_{t\to+\infty} \|l(t)\| \le l_\infty, \text{ and } \lim_{t\to+\infty} \|\tilde{\theta}(t)\| \le \tilde{\theta}_\infty, \qquad (3)$$

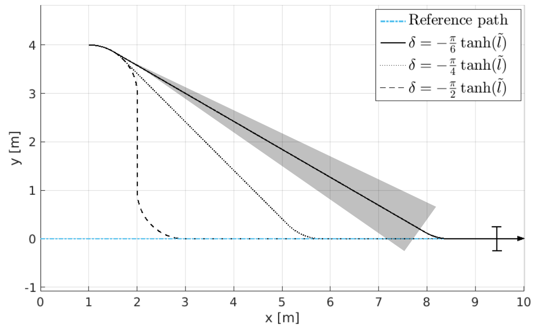

Fig. 3. Approach of a straight path with different δ angles. The shaded cone around the δ reference represents tolerable tracking errors that still guarantee path following, as explained in Section IV.

where $l_\infty \geq 0$ and $\tilde{\theta}_\infty \geq 0$ are positive arbitrary constants. The path is assumed to have a piecewise continuous and known curvature $c(s)$, i.e., comprising sequence of *clothoids*. A clothoid is a curve having curvature that is linear with respect to the arc length and it is given by $k(s) = \kappa + \frac{\mathrm{d}\kappa}{\mathrm{d}s}s$, where $\kappa \in \mathbb{R}$ is the curvature parameter. For example, straight linear segments and circular arcs are, indeed, special cases of clothoids [26]. This paper focuses only on the path following problem, then a free-obstacle path is assumed.

III. Fixed Curvature Controller with Chattering

The problem of driving a Dubins' car to a generic path by assuming a maximum known curvature for the path is solved in [19] using a hybrid controller and the path-related coordinates $(\tilde{l}, \tilde{\theta})$, where $\tilde{\theta}$ is the same as in (2), while $\tilde{l} = l/R$, with l as in (2) and R is the fixed maximum turning radius of the vehicle, i.e., half of the rear wheel axle length. The controller automaton comprises three manoeuvres, i.e., *Go Straight*, *Turn Right* and *Turn Left*, which are defined in terms of the angular velocity ω of (1) as

$$\begin{cases} \omega = 0, & \text{if } \textit{Go Straight}, \\ \omega = -\frac{v}{R}, & \text{if } \textit{Turn Right}, \\ \omega = \frac{v}{R}, & \text{if } \textit{Turn Left}, \end{cases} \tag{4}$$

assuming the forward input $v > 0$ uncontrollable but measurable. The working mode of the hybrid automaton is selected by partitioning the state space $(\tilde{l}, \tilde{\theta})$ into a set of non-overlapping regions. In each region only one of the three manoeuvres is active.

This strategy is generalised in [27] by the introduction of the *approaching path* governed by the *approaching angle* δ. δ varies according to the position of the vehicle with respect to the path and defines the way in which the vehicle approaches the path: for example, if $\delta = \pi/2$, the vehicle will approach the path perpendicularly (minimum path length), while if $\delta = 0$ the vehicle moves parallel to the path (see Figure 3 for reference). For the sake of completeness, the main result of [27] is reported next.

Theorem 1: For any function $\delta(\tilde{l})$ continuous, limited $\delta(\tilde{l}) \in (-\pi, \pi)$, with $-\mathrm{sign}(\tilde{l})\dfrac{\partial\delta(\tilde{l})}{\delta\tilde{l}} \geq 0$ and satisfying $\tilde{l}\delta(\tilde{l}) > 0$, $\forall \tilde{l} \neq 0$, the origin of the space $(\tilde{l}, \tilde{\theta})$ is asymptotically stable.

The rationale of Theorem 1 is that the limited ω set as defined in (4) can be used to let $\tilde{\theta}$ continuously track δ. Then, by letting $\delta(\tilde{l})$ be a continuous saturated odd function of $\tilde{l}$, the proof follows. For example, $\delta = -\theta_a \tanh(\tilde{l})$, where $\theta_a \in (0, \pi/2]$, guarantees vehicle asymptotic stability. In order to limit the number of corrections, an additional constraint is that

$$\|\dot{\delta}\| < \frac{v}{R}, \tag{5}$$

satisfied for $\delta = -\theta_a \tanh(\tilde{l})$ [27]. Constraint (5) guarantees that the approaching angle δ has a slower time variation than the maximum angular velocity of the vehicle. It has to be noted that for any $v > 0$, which for the *FriWalk* is provided by the user, we have perfect path following using the same arguments of [19].

However, the main problem of this solution is that a chattering control action is required to track paths with generic curvature greater than R^{-1}, which is unavoidable because of the ω constraints (4). Hence, albeit effective even in presence of a zero mean Gaussian noises affecting the angular velocity ω of the vehicle to simulate a user behaviour, this solution can only be tested in simulation. The simulative results showed that perfect path following can be achieved, but the commanded angular velocity ω almost surely chatters between the two turning manoeuvres of $\omega = \pm\frac{v}{R}$ (e.g., the vehicle braking system is activated more than 1700 times in 40 seconds for a path of 50 meters). Since this chattering phenomenon prevents the practical applicability of the controller to the *FriWalk*, we present in Section IV a hybrid formulation that overcomes this unbearable limit.

IV. Hybrid Controller Design for the *FriWalk*

In order to solve the path following problem (3) and maximise the user comfort, the goal is to limit as much as possible the braking system interventions. Strictly speaking, with respect to the control design (4), the controller we are aiming at should "most of the time" provide the *Go Straight* manoeuvre. Therefore, if the *FriWalk* is in the safety tunnel defined in (3), no control action is taken (*Go Straight*), otherwise the vehicle has to be controlled. This condition is captured by the logic variable p: if $p = 0$, the vehicle is in the safety tunnel, if $p = 1$, the vehicle is far apart and a control action should take place. Of course, the tighter is the safety tunnel, the smaller would be the tracking error. To further reduce the chattering phenomenon and the control authority, we noticed that, if the user is following the approaching angle δ with a certain tolerance that still guarantees the convergence towards the path, the *Go Straight* manoeuvre is again enforced. This condition is captured by the logic variable q: if $q = 0$, the vehicle is approaching the path with the given tolerance, if $q = 1$, the vehicle definitely needs a control action. Similarly to the logic variable p, the tighter is the tolerance, the higher would be the control authority. To rule the switching of the two logic variables, we defined the following function of the vehicle state ζ in (2):

$$T_p = \tilde{l}^2 + k_\theta^p\,\tilde{\theta}^2, \qquad T_q = k_\theta^q(\tilde{\theta} - \delta)^2, \tag{6}$$

with $k_\theta^q > 0$ and $k_\theta^p > 0$ tuning constants. In practice, when $T_p \le T_{p_1}$ ($T_{p_1} > 0$) the vehicle is inside the safety tunnel and hence $p = 0$. If $T_p \ge T_{p_2}$ ($T_{p_2} > T_{p_1} > 0$), $p = 1$. If $T_p \in (T_{p_1}, T_{p_2})$, the value of p depends on the past history, i.e., a hysteresis, in order to increase the robustness of the method to measurement noises and to further reduce the chattering. A similar behaviour is defined for the logic variable q with respect ot the thresholds $T_{q_2} > T_{q_1} > 0$ ($T_q \le T_{q_1} \Rightarrow q = 0$, $T_q \ge T_{q_2} \Rightarrow q = 1$).

To correctly model this complex switching behaviour, we resort to the theory of hybrid systems [28]. By defining the flow set $\mathcal{C} = \mathcal{C}_1 \cup \mathcal{C}_2 \cup \mathcal{C}_3 \cup \mathcal{C}_4$, where

$$\begin{aligned}
\mathcal{C}_1 &= \left\{\Theta \in \mathbb{R}^6, T_q \le T_{q_2} \ \wedge\ q = 0\right\},\\
\mathcal{C}_2 &= \left\{\Theta \in \mathbb{R}^6, T_q \ge T_{q_1} \ \wedge\ q = 1\right\},\\
\mathcal{C}_3 &= \left\{\Theta \in \mathbb{R}^6, T_p \le T_{p_2} \ \wedge\ p = 0\right\},\\
\mathcal{C}_4 &= \left\{\Theta \in \mathbb{R}^6, T_p \ge T_{p_1} \ \wedge\ p = 1\right\},
\end{aligned} \tag{7}$$

and $\Theta = [\chi^T, \omega, v, q, p]^T$ is the state of the hybrid system, and the jump sets $\mathcal{D}_q = \mathcal{D}_1 \cup \mathcal{D}_2$ and $\mathcal{D}_p = \mathcal{D}_3 \cup \mathcal{D}_4$, where

$$\begin{aligned}
\mathcal{D}_1 &= \left\{\Theta \in \mathbb{R}^6, T_q \ge T_{q_2} \ \wedge\ q = 0 \ \wedge\ p = 1\right\},\\
\mathcal{D}_2 &= \left\{\Theta \in \mathbb{R}^6, T_q \le T_{q_1} \ \wedge\ q = 1 \ \wedge\ p = 1\right\},\\
\mathcal{D}_3 &= \left\{\Theta \in \mathbb{R}^6, T_p \ge T_{p_2} \ \wedge\ p = 0\right\},\\
\mathcal{D}_4 &= \left\{\Theta \in \mathbb{R}^6, T_p \le T_{p_1} \ \wedge\ p = 1\right\},
\end{aligned} \tag{8}$$

we can finally have the following hybrid dynamic

$$\begin{cases}
\dot{\chi} = f(\Theta),\\
\dot{\omega} = p\,q\,g(\chi),\\
\dot{v} = h(\Theta),\\
\dot{q} = 0,\\
\dot{p} = 0,
\end{cases}
\quad
\begin{cases}
\chi^+ = \chi\\
\omega^+ = 0,\\
v^+ = v,\\
q^+ = p\,(1-q),\\
p^+ = p,
\end{cases}
\quad
\begin{cases}
\chi^+ = \chi,\\
\omega^+ = 0,\\
v^+ = v,\\
q^+ = q\,(1-p),\\
p^+ = 1-p,
\end{cases}$$
$$\Theta \in \mathcal{C} \qquad\qquad \Theta \in \mathcal{D}_q \qquad\qquad \Theta \in \mathcal{D}_p, \tag{9}$$

where the nonlinear function $g(\chi) \mapsto \{-\frac{v}{R}, 0, \frac{v}{R}\}$ is a static map that, given $(\tilde{\theta}, \tilde{l})$ returns the value of the angular velocity ω to steer $\tilde{\theta}$ towards $\tilde{l}$, as defined by Theorem 1. In practice, $g(\cdot)$ establishes which wheel has to be blocked, acting then as an impulsive function (this means that the wheel is blocked instantaneously). The function $h(\cdot)$ describes the dummy dynamics of the forward velocity v and, in general, depends on the user. Notice that the dynamics of v, which is a state variables of the hybrid system, is not needed as long as it is measurable.

Remark 1 (Interpretation of the logic variable p): The state p is initialised at $p(0) = 1$. When $p = 1$ (vehicle outside the safety tunnel), the third dynamic of (9) is only fired when $T_p \le T_{p_1}$ (see $\mathcal{D}_4$ in (8)), hence both q and p are set to zero. In this condition, the control can be reactivated only if p switches back to 1, which happens only if the condition of $\mathcal{D}_3$ in (8) is verified (hysteresis effect). In other words, closeness to the path in the sense of (6) rules on the control activation, as desired.

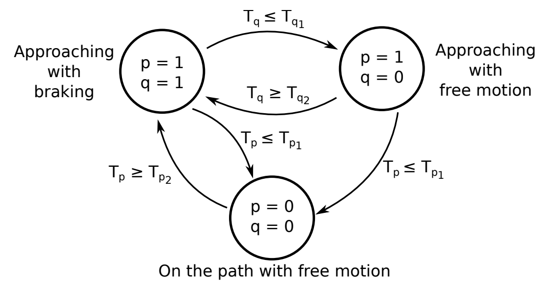

Fig. 4. Hybrid system states and switching conditions.

Remark 2 (Interpretation of the logic variable q): The state q is initialised at $q(0) = 0$. In light of Remark 1, the control can be activated only if $p = 1$. The second dynamic of (9) ensures a switch of q from 0 to 1 (braking system is attached) when condition of $\mathcal{D}_1$ in (8) is verified, or from 1 to 0 (braking system is detached) when instead condition of $\mathcal{D}_2$ in (8) is verified. In other words, the vehicle starts to rotate left or right (in the spirit of (4)) and does not switch directly from left to right, but there will be a finite time in which the *Go Straight* manoeuvre is activated. This is a direct consequence of the adoption of the approaching angle δ and motivates the choice of the manoeuvre made by $g(\cdot)$.

A. Analysis of the logical states jumps

The hybrid dynamics reported in (9) defines a hybrid automaton with three states, as depicted in Fig. 4. The discrete dynamics of the logical states p and q hence enjoy the following properties.

Property 1: The condition $[p, q] = [0, 1]$, i.e. the vehicle is controlled ($q = 1$) even if it is close to the path and correctly oriented ($p = 0$), never takes place.

If the initial condition has been wrongly set to $[p, q] = [0, 1]$ the discrete dynamics associated to $\mathcal{D}_p$ ensures $[p, q] = [1, 1]$.

Property 2: If $\Theta \in \mathcal{D}_p$ and $\Theta \in \mathcal{D}_q$ simultaneously, both the two discrete dynamics take place. The final value will be $[p, q] = [0, 0]$, regardless of execution order.

We are now in a position to prove the following convergence Theorem.

Theorem 2: Consider the system (1) subjected to the limitations (4) and two positive constants l_∞ and $\tilde{\theta}_\infty$. Choose δ as an odd function of $\tilde{l}$ satisfying (5). Then, there exist two constants T_{q_2} and T_{p_2} such that the hybrid controller (9) makes the path following requirement (3) to hold.

Proof: If $T_{q_1} = T_{q_2} = T_{p_1} = T_{p_2} = 0$, the controller is continuously activated. By applying the control laws in (4) and assuming that (5) holds, it is possible to steer the vehicle such that $\tilde{\theta} = \delta$ due to Theorem 1. By means of the Lyapunov function $V = \frac{1}{2}(\tilde{\theta}^2 + \tilde{l}^2)$ and its derivative

$$\dot{V} = \tilde{l}\,\frac{v}{R}\,\sin\tilde{\theta}, \tag{10}$$

and ensuring that δ is an odd function of $\tilde{l}$, we have that $\dot{V} \le 0$ and $\dot{V} = 0$ iff $\tilde{l} = 0$ [27]. This way, $\tilde{\theta} = 0$ and hence the path following requirement (3) is satisfied with $\tilde{\theta}_\infty = l_\infty = 0$.

Suppose $p = 1$. With thresholds different from zero and with condition (5) verified, the controller (4) ensures for $q = 1$ that $\dot{T}_q = 2k_\theta^q \left(\tilde{\theta} - \delta\right)(\omega - \dot{\delta}) < 0$. This happens since in such a case the vehicle either steers right or left to δ.

Recall that $\dot{V} \leq 0$ is indeed true if $\delta = \tilde{\theta}$, but also if

$$\|\tilde{\theta} - \delta\| \leq \epsilon, \tag{11}$$

where $\epsilon > 0$ is a sufficiently small constant. This condition is depicted by the shaded area in Figure 3: even if $\tilde{\theta}$ slightly differs from δ, the vehicle still approaches the path since it is pointing towards it, albeit with a different angle. This yields a great flexibility and robustness with respect to the approaching angle and, hence, reduces the number of braking actions. Therefore, since certainly $\dot{T}_q < 0$ when $T_q \geq T_{q_2}$ (i.e., *Approaching with braking* state of Figure 4), the hysteresis value T_{q_2} has just to be chosen sufficiently small to ensure that relation (11) holds. In practice, it is sufficient to ensure that the vehicle points towards the path when $T_q \leq T_{q_2}$ (i.e., *Approaching with free motion* state of Figure 4).

Whenever the Lyapunov function V decreases, T_p decreases as well, hence it will sooner or later reach $T_p \leq T_{p_1}$ and then $p = 0$, i.e., vehicle is in the safety tunnel around the path and no control action is applied. If T_p exceeds the hysteresis threshold T_{p_2}, it is not ensured that (10) is negative. However, since the control action restarts, the angle $\tilde{\theta}$ tends to δ and (10) will become negative semidefinite as before. As a consequence, in the transient phase, i.e., when $\tilde{\theta}$ tends to δ, the Lyapunov function V may reach in the worst case a maximum value $\overline{V}$. By simple geometric analysis (i.e., the vehicle constantly turns with the minimum turning radius on the left or on the right), it turns out that $\overline{V}$ is proportional to T_{p_2} and $\overline{V} = 0$ if $T_{p_2} = 0$. As a consequence, given l_∞ and $\tilde{\theta}_\infty$, it is immediate to choose T_{p_2} sufficiently small to make (3) holds.

■

V. Results

The effectiveness of the proposed solution has been firstly tested via simulations. Figure 5 reports the path tracked by the vehicle starting with an initial configuration $(x, y, \theta) = (1\text{ m}, 8\text{ m}, 0\text{ rad})$. The final position of the robot on the path is highlighted with a dashed circle. The function $\delta(\tilde{l}) = \frac{\pi}{2}\tanh(\tilde{l})$ is adopted, while a fixed dummy values of velocity $v = 1$ m/s is used. Notice how the vehicle changes direction according to the braking action fired by the threshold T_{p_2} defining the safety tunnel. This tunnel is also depicted in Figure 5: notice how the vehicle is corrected by the braking action whenever it reaches its boundaries. Since T_{p_2} depends on the states $\tilde{l}$ and $\tilde{\theta}$, the tunnel is a circle centered in the origin in the plane $(\tilde{l}, \tilde{\theta})$. As a consequence, the tunnel width is state dependent in the plane (x, y).

The time evolution of the coordinates l and $\tilde{\theta}$ of system (2) are reported in Figure 6-(a,b), respectively, while Figure 6-(c,d) depicts the time evolution of the variables T_p and T_q

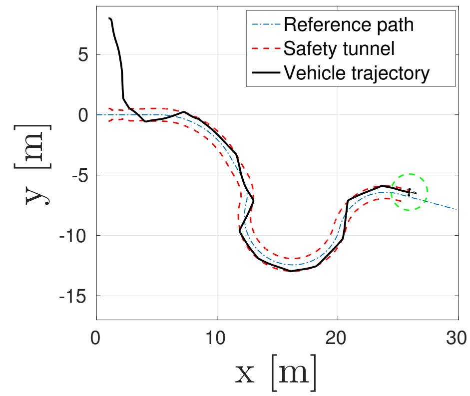

Fig. 5. Path following of a generic path. The reference (dash dotted line), the safety tunnel (dashed lines) and the vehicle trajectory (solid line) are reported. The vehicle final position is highlighted with a circle.

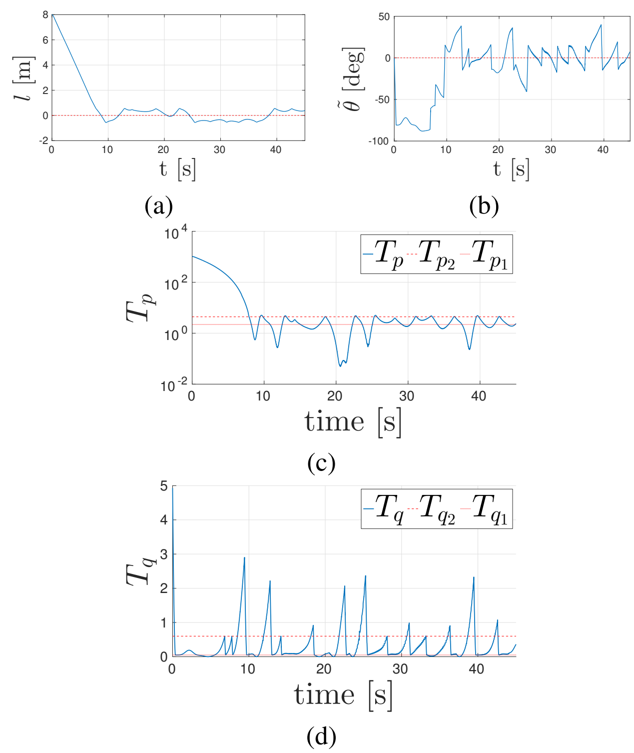

Fig. 6. Time evolution of the variables l (a), $\tilde{\theta}$ (b), T_p with thresholds T_{p_1} and T_{p_2} (c), and T_q with thresholds T_{q_1} and T_{q_2} (d) for the trajectory depicted in Figure 5.

defined in (6) compared with the corresponding threshold values. Notice how the control action is governed by the threshold T_p, which implies that T_q may occasionally exceed its own threshold if the vehicle is close enough to the path. The sharp variations in all the graphs are a consequence of the bang-bang braking action. Finally notice that the $\tilde{\theta}$ time evolution is affected by the presence of a Gaussian noise superimposed to the vehicle dynamics when it is in the *Go Straight* manoeuvre.

To better highlight the effect of the controller on the chattering phenomenon, Figure 7-(a) shows the number of braking actions as a function of the threshold values T_{p_1}

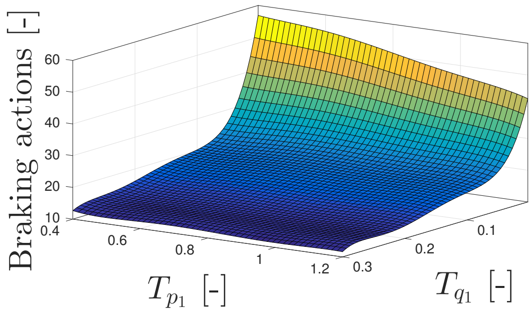

(a) Number of braking actions.

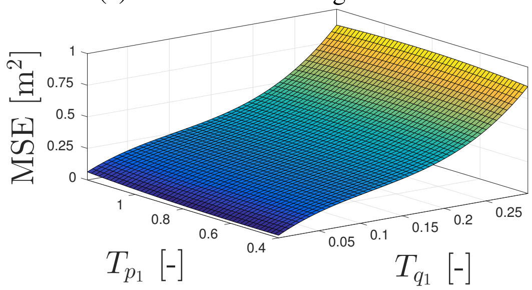

(b) Mean square error.

Fig. 7. Influence of hystereses thresholds on the number of braking actions (a) and on the MSE of the path following (b). The surfaces are obtained by interpolating more than 500 points computed via simulations. Each point is obtained with a mean of five simulations.

and T_{q_1} (the upper values of the hystereses are chosen by setting $T_{p_2} = 2T_{p_1}$ and $T_{q_2} = 2T_{q_1}$, respectively). Notice that, the larger T_{p_1} and T_{q_1}, the smaller is the number of braking actions. As described in Section IV, the threshold T_{q_1} modifies the authority of the controller, and hence has a radically more evident impact on the number of braking actions, and, hence, on the user comfort. In contrast, the larger T_{p_1} and T_{q_1}, the larger is the Mean Squared Error (MSE), i.e., the mean of the steady state squared distances l^2 from the path. Again, the value of T_{q_1} has an higher impact on the MSE since it rules the controller authority.

A. Experimental Results

The hybrid braking system has been implemented and tested on the *FriWalk*. The experimental set-up has the following features:

- To let the user completely relying on the braking system guidance, he/she receives no prior information on the path to follow. The user starts from $(x, y, \theta) = (-0.8 \text{ m}, -0.3 \text{ m}, \pi/4 \text{ rad})$, which is outside the safety tunnel (see Figure 8);
- The sensors adopted to localize the cart in the environment are encoders mounted on the rear wheels and a camera rigidly fixed to the chassis. The camera points on the floor where QR-codes are placed, whose positions and orientations in the map are known a priori. Therefore, the camera provides an absolute measure of the walker position and orientation, while the odometry (i.e., the localisation of the vehicle based on the encoders data) provides an incremental measure with increasing uncertainty (i.e., dead reckoning). However, the camera can be used only if a QR-code is sensed, while the odometry data are always available. The implemented localisation algorithm combines the odometry and the camera measures as described in [21];
- As aforementioned, the actuators are the brakes mounted on the rear wheels. The physical inputs are the currents commanded to the brakes. The commanded currents vary form 40 mA to 250 mA. When the current equals 250 mA, the wheel is blocked. From practical evidence, the minimum value of 40 mA corresponds to an almost zero breaking torque (not perceived by the user) and reduces the settling time of the current;
- The hystereses parameters are set to $T_{q_1} = 0.2$, $T_{q_2} = 0.5$, $T_{p_1} = 0.1$, $T_{p_2} = 0.3$, $k_\theta^q = 2$ and $k_\theta^p = 1$. As a rule of thumb for tuning, T_{q_1}, T_{q_2} and k_θ^q determine when the control actions are applied in the presence of orientation errors only (i.e., when the difference $\|\tilde{\theta} - \delta\|$ is large), while T_{p_1}, T_{p_2} and k_θ^p determine when the user is sufficiently close to the path (both in terms of distance and orientation) and, hence, no control action is required.

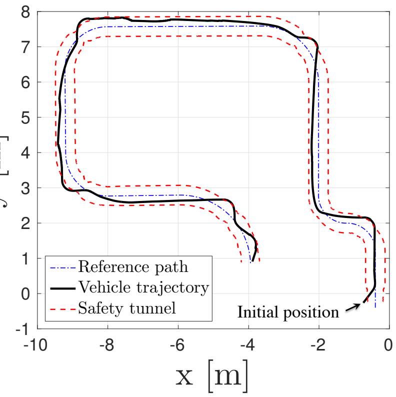

Fig. 8. Experimental following of a generic path. The reference (dash dotted line), the safety tunnel (dashed lines) and the actual vehicle trajectory (solid line) are reported.

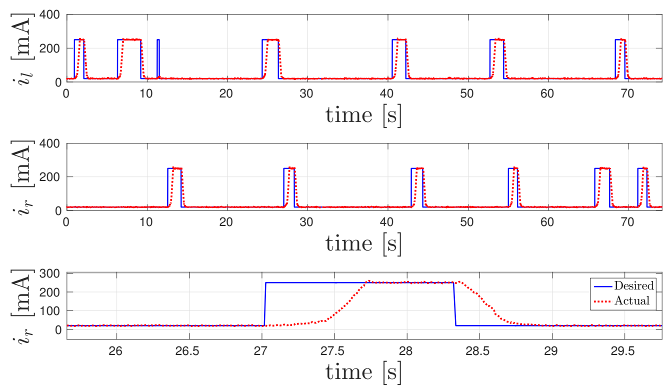

Fig. 9. Experimental behaviour of right and left brake currents.

Figure 8 reports the path followed by the user, while Figure 9 shows the currents applied on the electromechanical brakes. The number of peaks in Figure 9 coincide with the number of braking actions applied by the hybrid controller.

Notice that, due to manufacturing properties, the actuation of the brakes takes place with a delay (bottom plot of Figure 9). This delay affects the steering behaviour of the vehicle (Figure 8), by prolonging the uncontrolled *Go Straight* manoeuvre and, hence, requiring a longer braking action. This is the reason way occasionally, the vehicle exceeds the safety tunnel. When the braking action is released, a similar effect takes place, but the delay is smaller and hence a lighter effect on the path following accuracy can be noticed. Due to the tolerance imposed by T_p, a motion of the vehicle almost parallel to the path is allowed providing that the distance is limited, hence increasing the user comfort (no useless braking actions are applied). Finally, notice the perfect accordance of results between the simulations and the experiments.

VI. Conclusions

In this paper we have presented a hybrid control strategy for a robotic walking assistant controlled with a passive braking system. Due to cost limits and mechanical simplicity, the walker is not endowed with force sensors, hence the proposed solution is based on a simple actuation strategy in which the braking system is controlled with a bang-bang approach. We have shown, through simulations and experiments, that it is possible to secure a gentle and smooth path following by limiting the number of braking actions and avoiding the chattering phenomenon. Tuning parameters acting on the tracking accuracy and on the control authority are also exposed in the current controller implementation. In the experimental analysis, the main problem is the delay of the brake actuation, which causes more interventions of the controller than necessary. This delay is not considered by the controller since the function $g(\cdot)$ in (9) is impulsive.

Future developments will focus on the compensation of the hardware delay, in order to reduce the annoying switching among the different states during the curves. Another point that serves some further investigations is related to the user behaviour in the *go Straight* manoeuvre that should be sustained by the synergistic use of visual and/or audio feedback.

References

[1] L. Hedley, N. Suckley, L. Robinson, and P. Dawson, "Staying steady: a community-based exercise initiative for falls prevention," *Physiotherapy theory and practice*, vol. 26, no. 7, pp. 425–438, 2010.

[2] K.-T. Khaw, N. Wareham, S. Bingham, A. Welch, R. Luben, N. Day *et al.*, "Combined impact of health behaviours and mortality in men and women: the epic-norfolk prospective population study," *Obstetrical and Gynecological Survey*, vol. 63, no. 6, pp. 376–377, 2008.

[3] "ACANTO: A CyberphysicAl social NeTwOrk using robot friends," http://www.ict-acanto.eu/acanto, February 2015, EU Project.

[4] A. Goswami, M. Peshkin, and J. Colgate, "Passive robotics: An exploration of mechanical computation," in *Proceedings of the 1990 American Control Conference*, 1990, pp. 2791–2796.

[5] M. Saida, Y. Hirata, and K. Kosuge, "Pose estimation of servo-brake-controlled caster units arbitrarily located on a mobile base," in *IEEE/RSJ International Conference on Intelligent Robots and Systems (IROS)*, Sept 2014, pp. 3456–3462.

[6] ——, "Motion control of caster-type passive mobile robot with servo brakes," *Advanced Robotics*, vol. 26, no. 11-12, pp. 1271–1290, 2012.

[7] R. Gillespie, J. Colgate, and M. Peshkin, "A general framework for Cobot control," *IEEE Transactions on Robotics and Automation*, vol. 17, no. 4, pp. 391–401, 2001.

[8] K. Wakita, J. Huang, P. Di, K. Sekiyama, and T. Fukuda, "Human-Walking-Intention-Based Motion Control of an Omnidirectional-Type Cane Robot," *IEEE/ASME Transactions on Mechatronics*, vol. 18, no. 1, pp. 285–296, Feb 2013.

[9] S. Suzuki, Y. Hirata, K. Kosuge, and H. Onodera, "Motion support during the swing phase using cooperative walking support system," *Advanced Robotics*, vol. 27, no. 17, pp. 1337–1349, 2013.

[10] Y. Hirata, K. Kosuge, and E. Monacelli, "Steering assist system for a cycling wheelchair based on braking control," in *IEEE/RSJ International Conference on Intelligent Robots and Systems (IROS)*, Nov 2013, pp. 672–678.

[11] Y. Hirata, A. Hara, and K. Kosuge, "Motion control of passive intelligent walker using servo brakes," *IEEE Transactions on Robotics*, vol. 23, no. 5, pp. 981–990, 2007.

[12] T. Pilutti, G. Ulsoy, and D. Hrovat, "Vehicle steering intervention through differential braking," in *Proceedings of the 1995 American Control Conference*, vol. 3, 1995, pp. 1667–1671.

[13] M. Saida, Y. Hirata, and K. Kosuge, "Development of passive type double wheel caster unit based on analysis of feasible braking force and moment set," in *Proceedings of the 2011 IEEE/RSJ International Conference on Intelligent Robots and Systems*, 2011, pp. 311–317.

[14] Y.-H. Hsieh, K.-Y. Young, and C.-H. Ko, "Effective maneuver for passive robot walking helper based on user intention," *IEEE Transactions on Industrial Electronics*, vol. 62, no. 10, pp. 6404–6416, Oct 2015.

[15] D. Fontanelli, A. Giannitrapani, L. Palopoli, and D. Prattichizzo, "Unicycle Steering by Brakes: a Passive Guidance Support for an Assistive Cart," in *Proc. IEEE Int. Conf. on Decision and Control*. Florence, Italy: IEEE, 10-13 Dec. 2013, pp. 2275–2280.

[16] ——, "A Passive Guidance System for a Robotic Walking Assistant using Brakes," in *Proc. IEEE Int. Conf. on Decision and Control (CDC)*. Osaka, Japan: IEEE, 15-18 Dec. 2015, pp. 829–834.

[17] A. Balluchi, A. Bicchi, A. Balestrino, and G. Casalino, "Path tracking control for dubin's cars," in *Proc. IEEE Conf. on Robotics and Automation (ICRA)*, vol. 4, Apr 1996, pp. 3123–3128.

[18] P. Soueres, A. Balluchi, and A. Bicchi, "Optimal feedback control for route tracking with a bounded-curvature vehicle," *International Journal of Control*, vol. 74, no. 10, pp. 1009–1019, 2001.

[19] A. Balluchi, A. Bicchi, and P. Soueres, "Path-following with a bounded-curvature vehicle: a hybrid control approach," *International Journal of Control*, vol. 78, no. 15, pp. 1228–1247, 2005.

[20] P. Nazemzadeh, D. Fontanelli, D. Macii, T. Rizano, and L. Palopoli, "Design and Performance Analysis of an Indoor Position Tracking Technique for Smart Rollators," in *International Conference on Indoor Positioning and Indoor Navigation (IPIN)*. Montbeliard, France: IEEE GRSS, 28-31 Oct. 2013, pp. 1–10.

[21] P. Nazemzadeh, F. Moro, D. Fontanelli, D. Macii, and L. Palopoli, "Indoor Positioning of a Robotic Walking Assistant for Large Public Environments," *IEEE Trans. on Instrumentation and Measurement*, vol. 64, no. 11, pp. 2965–2976, Nov 2015.

[22] A. Colombo, D. Fontanelli, A. Legay, L. Palopoli, and S. Sedwards, "Motion planning in crowds using statistical model checking to enhance the social force model," in *Decision and Control (CDC), 2013 IEEE 52nd Annual Conference on*. IEEE, 2013, pp. 3602–3608.

[23] ——, "Efficient customisable dynamic motion planning for assistive robots in complex human environments," *Journal of Ambient Intelligence and Smart Environments*, vol. 7, no. 5, pp. 617–633, 2015.

[24] J.-P. Laumond, *Robot motion planning and control. Lectures Notes in Control and Information Sciences 229*, 1998, vol. 3.

[25] J. P. Hespanha and A. S. Morse, "Switching between stabilizing controllers," *Automatica*, no. 38, pp. 1905–1917, June 2002.

[26] M. Frego, E. Bertolazzi, F. Biral, D. Fontanelli, and L. Palopoli, "Semi-Analytical Minimum Time Solutions for a Vehicle Following Clothoid-Based Trajectory Subject to Velocity Constraints," in *European Control Conference*, Aalborg, Denmark, July 2016, accepted.

[27] M. Andreetto, S. Divan, D. Fontanelli, and L. Palopoli, "Hybrid Feedback Path Following for Robotic Walkers via Bang-Bang Control Actions," in *Proc. IEEE Int. Conf. on Decision and Control (CDC)*. Las Vegas, USA: IEEE, 2016, accepted.

[28] R. Goebel, R. G. Sanfelice, and A. R. Teel, *Hybrid Dynamical Systems: modeling, stability, and robustness*. Princeton University Press, 2012.